Active quasi-circulator realisation with gain elements and slow-wave couplers

C.E. Saavedra and Y. Zheng

Abstract: A microstrip active quasi-circulator is presented using two generic amplifier blocks and two power couplers. The power couplers are parallel-coupled lines with a slow-wave structure in order to improve the isolation between ports of the quasi-circulator. A detailed analytic design procedure is presented for the slow-wave couplers based on the capacitive coupling modelling approach for coupled transmission lines. Experimental results show that the quasi-circulator has an insertion loss between 1 and −2 dB, a return loss better than 11 dB at each of the ports and an isolation better than 20 dB from 1.0 to 3.0 GHz. The input 1 dB compression point is 14 dB m at 2.4 GHz.

1 Introduction

Circulators are three-port non-reciprocal devices in which the incident signal at one port circulates in a single direction, for instance, clockwise, towards the next port. Non-adjacent ports are isolated from each other. These circuits can separate an incident wave from a reflected wave and thus can be used in reflection amplifiers [1] and reflection phase shifters [2], for example. Circulators are also used for duplexing in radio systems to allow an antenna to be shared between a transmitter and a receiver [3].

Most circulators currently in use are passive and they are made using ferrite materials, which make them costly, and they are not compatible with monolithic integration. To eliminate the use of ferrites, there have been several investigations into active circulators realised with transistors and gain elements.

In [4], an active circulator was demonstrated using three transistors and it had an upper frequency cutoff of 3 MHz. Later in [5], a similar topology to that in [4] was used and the frequency response was extended to 2.1 GHz with an insertion loss of 6 dB and an isolation of 18 dB.

In [6], a unilateral out-of-phase power divider realised using an active balun was used together with a GaAs FET in-phase power combiner to make an active quasi-circulator. A quasi-circulator is a simplified version of a circulator in which there is a power transfer from port 1 to port 2, and from port 2 to port 3, but there is no power transfer from port 3 to port 1. The circuit in question had a wideband response, an insertion loss of about 5 dB and an isolation higher than 15 dB over the band. Three quasi-circulators were later used to make a complete circulator circuit, at the expense of larger chip area.

In [7], an active circulator is shown which uses three amplifiers in a ring configuration and there is a power coupler at the junction between amplifiers. Lastly, a narrowband integrated active circulator antenna was proposed in [8] for use in transmit–receive applications. That circulator was a hybrid circuit implemented using a set of amplifiers also in a ring configuration.

In this work, a novel microstrip active quasi-circulator is proposed which uses two generic amplifier blocks and two power couplers with a slow-wave structure in order to improve the port-to-port isolation of the quasi-circulator. The isolation and the return loss are very good, and they are better than 20 and 11 dB, respectively, from 1.0 to 3.0 GHz. Although the other works surveyed do not present the power performance of their active circulators, in this work the input 1-dB compression point has been characterised and it is 14 dBm. This paper is organised as follows. Section 2 presents the circuit concept, Section 3 gives a detailed design procedure for the slow-wave couplers, Section 4 presents the experimental results and Section 5 concludes the work.

2 Quasi-circulator circuit description

A diagram of the proposed active quasi-circulator is shown in Fig. 1. The signal enters the circuit at port 1, whereupon it encounters a set of parallel-coupled lines with a slow-wave structure. The coupled line design will be discussed in more detail at a later point. Some of the incident energy will be coupled to the second transmission line and it will enter the first amplifier where the signal will be amplified and eventually exit at port 2. In order to achieve a 0 dB insertion loss from port 1 to port 2 (S_{21}), the amplifier gain must be equal to the coupling factor of the first set of coupled lines, so that the two quantities balance each other out. When the signal from amplifier 1 enters the second set of coupled lines, a small amount of energy will be coupled to its second transmission line and it will be absorbed by the 50-Ω load.

Now suppose that the incident signal enters the circulator at port 2. In this case, the energy will be coupled in the second set of coupled lines and the coupled signal will be amplified by amplifier 2 and eventually exit at port 3. Again, to achieve a 0 dB insertion loss for S_{32}, the gain of amplifier 2 must equal the coupling factor of the coupled lines.

In this active quasi-circulator circuit, the first coupler is needed in order to improve the isolation from port 2 to

doi:10.1049/iet-map:20060176

Paper first received 26th July 2006 and in revised form 14th May 2007

The authors are with the Department of Electrical and Computer Engineering, Queen's University, 410 Walter Light Hall, Kingston, Ont., K7L 3N6 Canada

E-mail: carlos.saavedra@queensu.ca

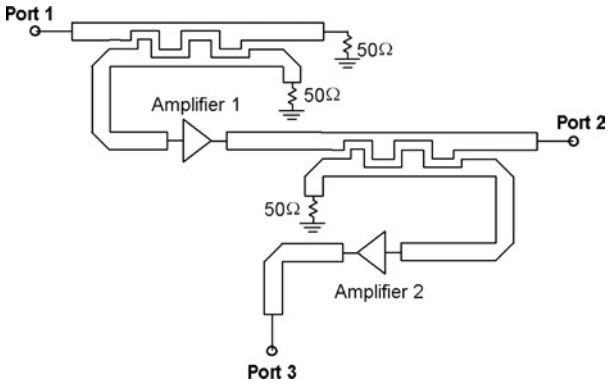

Fig. 1 *Proposed active quasi-circulator*

port 1 (S_{12}) since in this case S_{12} is determined by two quantities: (a) the reverse transmission coefficient of amplifier 1 and (b) the coupling factor of the first coupler. When added together, these two factors lead to a high isolation between port 2 and port 1.

The isolation from port 3 to port 2 (S_{23}) depends on the reverse transmission coefficient of amplifier 2 and on the coupling factor of the second pair of coupled lines. Since these quantities are similar to those of amplifier 1 and the first coupler, it is expected that S_{32} will be close to S_{12}, which is verified by experiment in Section 4.

The factors that determine the isolation from port 1 to port 3 (S_{31}) are different from the previous two cases and require special attention. The signal propagating from port 1 to port 3 goes through the first coupler and amplifier and it emerges with a 0 dB insertion loss as it enters the second coupler. At the second coupler, some energy goes to the coupled port, where it is primarily dissipated in the 50-Ω load, but some leakage energy reaches the isolated port of the coupler. This leakage energy is subsequently amplified by amplifier 2 and it ultimately reaches port 3. Therefore in order to have a high isolation between port 1 and port 3 of the active quasi-circulator, it is critical for the second coupler itself to have a high isolation. To achieve a high isolation, a slow-wave coupling structure is used.

It is well known that in a pair of common microstrip coupled lines, such as the ones in Fig. 2*a*, the even and the odd modes propagating through the structure travel at different phase velocities [9]. This is caused by the fact that the even and the odd modes see different effective dielectric constants and hence they propagate at different speeds. The result is that if energy is incident at port 1 in Fig. 2*a*, then port 3 will not be completely isolated as predicted by theory, but instead there will be a certain amount of leakage energy that reaches that port. To reduce this effect, a coupler with a slow-wave structure such as the one shown in Fig. 2*b* can be used [10, 11].

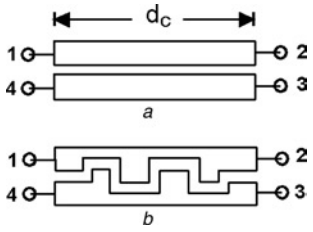

Fig. 2 *Microstrip coupled lines*

a Common type
b Slow-wave structure

Given that the slow-wave coupler is critical for the performance of the quasi-circulator in this work, Section 3 will present a detailed analytic design procedure for coupler.

The power performance of this active quasi-circulator is fundamentally determined, of course, by the characteristics of the amplifier circuits. It is interesting to note that in this circuit, if the insertion loss between the adjacent ports is 0 dB, then the input 1-dB compression point of the quasi-circulator will equal the output 1-dB compression point of the amplifier used. This is because the gain of the amplifiers will compensate the coupling loss of the power couplers, which allows for relatively high input power levels.

3 Slow-wave coupler design

The best way to analyse the operation of the slow-wave structure in Fig. 2*b* is to consider how the extra path length introduced by the meander in the inner edges of the coupled lines contributes to the fringing capacitance of the parallel transmission lines. The fringing capacitance has an effect on the odd-mode effective dielectric constant and thereby on the odd-mode phase velocity [11]. This approach has the benefit that it lends itself conveniently to analytic calculation and one can make a reasonably accurate prediction as to the enhancement of the isolation, $|S_{31}|$, of the slow-wave coupler with respect to the common coupler.

The even- and odd-mode effective dielectric constants and thus the even- and odd-mode phase velocities and impedances of the common coupler in Fig. 2*a* can be determined by the self and mutual capacitances between the two transmission lines. The total even- and odd-mode capacitances per unit length are given by [12]

$$\text{even mode:} \quad C_e = C_p + C_f + C'_f \tag{1}$$

$$\text{odd mode:} \quad C_o = C_p + C_f + C_{ga} + C_{gd} \tag{2}$$

For the even-mode capacitance, C_p is the parallel-plate capacitance between the microstrip lines and the ground plane, C_f the fringing capacitance on the outer edges of the transmission lines and C'_f the fringing capacitance on the inner edges. For the odd-mode capacitance, C_p and C_f are the same as before, C_{ga} is the fringing capacitance on the inner edges in the air dielectric and C_{gd} is also the fringing capacitance on the inner edges but in the substrate dielectric. Analytic expressions for calculating all of these capacitances are found in [12] and they depend only on the following input variables: the width and the separation of the transmission lines, the relative dielectric constant of the substrate and the thickness of the substrate. Using C_e and C_o from above, the even- and odd-mode effective dielectric constants in the coupler are found using the expressions

$$\text{evenmode:} \quad \varepsilon^{e}_{eff} = \frac{C_e}{C^{air}_e} \tag{3}$$

$$\text{oddmode:} \quad \varepsilon^{o}_{eff} = \frac{C_o}{C^{air}_o} \tag{4}$$

where C^{air}_e and C^{air}_o are the capacitances calculated with (1) and (2) but for a substrate having a relative dielectric constant of 1.0 (i.e. air).

For the slow-wave coupler of Fig. 2*b*, the even-mode capacitance is approximately the same as (1) but the odd-mode capacitance is larger because the meandering path increases the fringing fields in the inner edges of the coupler by an amount directly proportional to the path

length. The new odd-mode capacitance is therefore

$$C_{os} = C_p + C_f + \frac{d_s}{d_c}(C_{ga} + C_{gd}) \tag{5}$$

where d_s is the total path length of the slow-wave coupler along the centre line including the meander and d_c is the total length of the common coupler of Fig. 2*a*. For the slow-wave coupler, the odd-mode effective dielectric constant needs to be recalculated by using C_{os} in place of C_o in (4). Note that since $C_{os} > C_o$, the odd-mode effective dielectric constant becomes larger for the slow-wave coupler with respect to the common coupler and therefore the phase velocity of the odd-mode wave is slowed down.

The isolation, $|S_{31}|$, of the common coupler can be obtained by first calculating the $\boldsymbol{Z}$-parameter matrix of the four-port network as detailed in [13] and then converting the $\boldsymbol{Z}$-matrix into the $\boldsymbol{S}$-parameter matrix using the relationship

$$\boldsymbol{S} = (\boldsymbol{Z} - z_o\boldsymbol{U})(\boldsymbol{Z} + z_o\boldsymbol{U})^{-1} \tag{6}$$

where z_o is the characteristic impedance of the system, 50 Ω in this work, and $\boldsymbol{U}$ is the identity matrix. To predict the isolation of the slow-wave coupler, we make use of the fact that the isolation of any pair of coupled lines is given by [14]

$$I = |S_{31}| = \gamma\left(\frac{k_L - k_C}{k_L + k_C}\right) \tag{7}$$

where γ is a proportionality constant and k_L and k_C are the inductive and capacitive coupling coefficients, respectively, between the coupled lines. These two coupling coefficients are calculated using [15]

$$k_L = \frac{1 - C_e^{air}/C_o^{air}}{1 + C_e^{air}/C_o^{air}} \tag{8}$$

$$k_C = \frac{1 - \varepsilon_{eff}^{e} C_e^{air}/\varepsilon_{eff}^{o} C_o^{air}}{1 + \varepsilon_{eff}^{e} C_e^{air}/\varepsilon_{eff}^{o} C_o^{air}} \tag{9}$$

For the common coupler of Fig. 2*a*, γ is found by first calculating $|S_{31}|$ using (6) and then equating that result to (9) and solving for γ. This value of γ is subsequently used to calculate the isolation of the slow-wave coupler using (7).

Using the procedure described above the isolation, $|S_{31}|$ was calculated theoretically for the common coupler and for the slow-wave coupler. To verify the accuracy of the theoretical approach, full-wave electromagnetic simulations using the field solver momentum were performed on both couplers. Fig. 3*a* shows the response of the common coupler and Fig. 3*b* is the response of the slow-wave coupler. At 3.0 GHz, the isolation of the common coupler is 20.9 dB, whereas for the slow-wave coupler the isolation is 33.6 dB, an improvement of 12.7 dB. The coupling coefficient, $|S_{41}|$, for both the common and slow-wave couplers is about 10 dB. In this work, the length of the common coupler is $d_c = 9$ mm and the total inner path length of the slow-wave coupler is $d_s = 13$ mm. The gap between the transmission lines for both couplers is identical at 0.3 mm. The substrate has a thickness of 1.27 mm and its relative dielectric constant is 10.5.

4 Experimental results

The circuit in Fig. 1 was realised in microstrip with surface-mount gain blocks (Gali-2+) from Mini-Circuits and they had a gain of about 12 dB and reverse transmission of about 20 dB between 1.0 and 3.0 GHz.

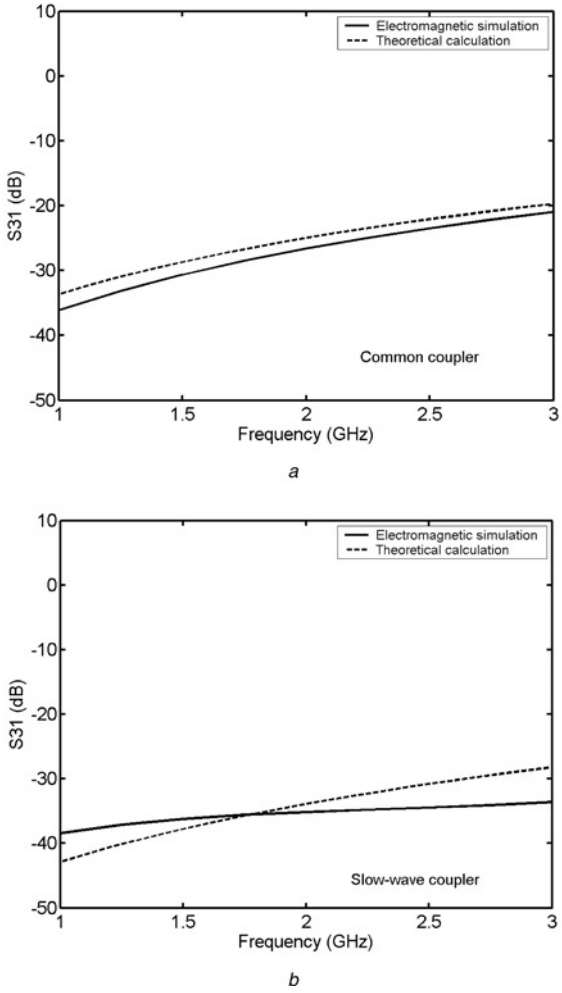

Fig. 3 *Theoretical and simulated isolation, $|S_{31}|$*
a Common coupler
b Slow-wave coupler

The quasi-circulator's measured insertion loss and reflection coefficients are shown in Fig. 4. It is seen that S_{21} and S_{32} are in the range +1 to −2 dB from 1.0 to 3.0 GHz. The reflection coefficients are better than −11 dB over the same band.

The isolation between the various ports is shown in Fig. 5. For S_{12} and S_{23}, the isolation was expected to be better than 30 dB because the reverse transmission of the amplifiers was 20 dB from 1.0 to 3.0 GHz and the coupling factor of the couplers was about 10 dB. It is observed experimentally that S_{12} and S_{23} are indeed both below −30 dB

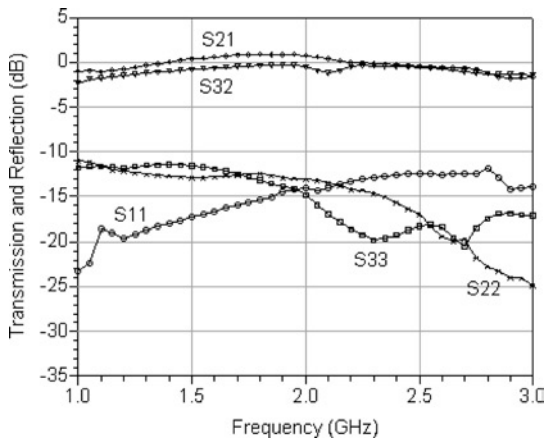

Fig. 4 *Measured insertion loss and reflection coefficients*

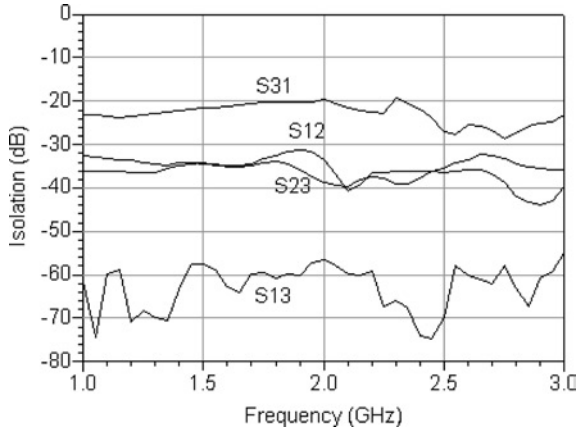

Fig. 5 *Isolation between the different ports of the quasi-circulator*

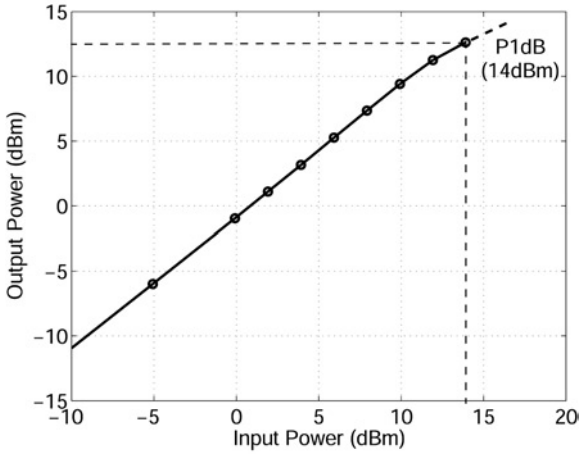

Fig. 6 *Quasi-circulator measured output power against input power at 2.4 GHz*

and their frequency responses are very close to each other. This was to be expected because the signal paths between port 2 and port 1 and between port 3 and port 2 are similar, as explained in Section 2. The isolation between port 1 and port 3 in the forward direction, S_{31}, is below -20 dB, which is in the neighbourhood of what is usually obtained with ferrite-based circulators. This value of S_{31} was possible by the use of the slow-wave structure in the coupled lines because the leakage energy in the second coupler was noticeably reduced. Finally, the reverse isolation between ports 1 and 3 (S_{13}) is excellent at around 60 dB, because in that direction, the signal path involves two amplifiers in the reverse direction (20 dB + 20 dB = 40 dB) and two couplers (10 dB + 10 dB = 20 dB).

A plot of the power performance of the quasi-circulator is shown in Fig. 6. The input 1 dB compression point was measured to be 14 dB m at 2.4 GHz, which is very close to the output 1-dB compression point of the amplifiers, as expected. A photograph of the circuit is shown in Fig. 7.

5 Conclusion

In this work, a novel active quasi-circulator hybrid circuit has been proposed and experimentally demonstrated. The

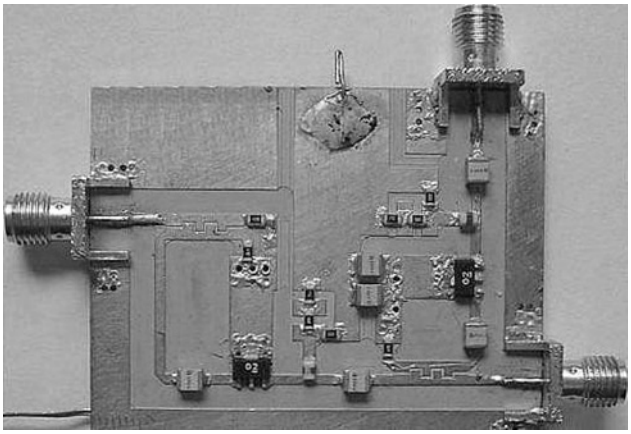

Fig. 7 *Photograph of the active quasi-circulator*

circuit operates between 1.0 and 3.0 GHz, has an insertion loss between the ports of approximately 0 dB, a return loss of 11 dB or better and an isolation better than 20 dB. The input 1-dB compression point is seen to be equal to the output 1-dB compression point of the amplifiers used. The use of slow-wave couplers was critical for the performance of this quasi-circulator since it made the isolation between ports 1 and 3 similar to what is obtained with ferrite circulators.

6 References

1 Steer, M.B.: 'Gain saturation in circulator-coupled reflection amplifiers'. IEEE MTT-S Int. Microwave Symp. Digest, St. Louis, MO, June 1985, pp. 395–398
2 Lucyszyn, S., and Robertson, I.D.: 'Decade bandwidth MMIC analogue phase shifter'. IEE Colloquium on Multi-Octave Microwave Circuits, November 1991, pp. 2/1–2/6
3 Chang, K.: 'Microwave passive and antenna components' (Wiley, New York, 1989), vol. 1, p. 253
4 Tanaka, S., Shimomura, N., and Ohtake, K.: 'Active circulators – the realization of circulators using transistors', *Proc. IEEE*, 1965, **3**, (3), pp. 260–267
5 Smith, M.A.: 'GaAs monolithic implementation of active circulators'. IEEE MTT-S Int. Microwave Symp. Digest, May 1988, pp. 1015–1015
6 Hara, S., Tokumitsu, T., and Aikawa, M.: 'Novel unilateral circuits for MMIC circulators', *IEEE Trans. Microw. Theory Technol.*, 1990, **38**, (10), pp. 1399–1406
7 Bahl, J.: 'The design of a 6-port active circulator'. IEEE MTT-S Int. Microwave Symp. Digest, May 1988, pp. 1011–1014
8 Cryan, M.J., and Hall, P.S.: 'An integrated active circulator antenna', *IEEE Microw. Guided Wave Lett.*, 1997, **7**, (7), pp. 190–191
9 Mongia, R., Bahl, I., and Bhartia, P.: 'RF and microwave coupled-line circuits' (Artech House, Boston, 1999)
10 Podell, A.: 'A high directivity microstrip coupler technique'. IEEE MTT-S Int. Microwave Symp. Digest, May 1970, pp. 33–36
11 Uysal, S.: 'Nonuniform line microstrip directional couplers and filters' (Artech House, Boston, 1993)
12 Garg, R., and Bahl, I.J.: 'Characteristics of coupled microstriplines', *IEEE Trans. Microw. Theory Technol.*, 1979, **27**, (7), pp. 700–705
13 Zysman, G.I., and Johnson, A.K.: 'Coupled transmission line networks in an inhomogeneous dielectric medium', *IEEE Trans. Microw. Theory Technol.*, 1969, **17**, (10), pp. 753–759
14 Krage, M.K., and Haddad, G.I.: 'Frequency-dependent characteristics of microstrip transmission lines', *IEEE Trans. Microw. Theory Technol.*, 1972, **20**, (10), pp. 678–688
15 Krage, M.K., and Haddad, G.I.: 'Characteristics of coupled microstrip transmission lines. II. Evaluation of coupled-line parameters', *IEEE Trans. Microw. Theory Technol.*, 1970, **18**, (4), pp. 222–228